doi: 10.4149/gpb_2025036

# Upregulation of SLC25A1 by MAZ reprograms fatty acid synthesis and fuels LUAD malignancy

Xiaomeng Li[1] and Jing Li[1]

[1] *Respiratory Medicine Center, Weifang People's Hospital, Weifang, China*

**Abstract.** Lung adenocarcinoma (LUAD) is a type of lung cancer with high incidence and mortality rates. Zinc finger protein 801 (MAZ) regulates cellular growth, proliferation, and differentiation, and its abnormal expression is associated with the occurrence of various tumors. In this study, the objective is to investigate the impact and underlying mechanism of MAZ on the malignant progression of LUAD. The expression of solute carrier family 25 member 1 (SLC25A1) was found to be elevated in LUAD, which indicated a relationship with a negative prognosis. Within LUAD cells, SLC25A1 was observed to not only boost proliferation but also hinder apoptosis and further augment fatty acid synthesis. MAZ, which was identified as the upstream regulator of SLC25A1, was also overexpressed in LUAD, thereby positively regulating the expression of SLC25A1. In addition, MAZ was found to accelerate the malignant behaviors of LUAD cells, specifically through its regulation of SLC25A1. Furthermore, *in vivo* studies confirmed that MAZ stimulated the malignant progression of LUAD *via* its influence on SLC25A1. In conclusions, MAZ mediates the upregulation of SLC25A1, which modifies the fatty acid synthesis pathway and fuels the malignant progression of LUAD. These findings suggest a new strategy for the targeting therapy in LUAD patients.

**Key words:** MAZ — SLC25A1 — Fatty acid synthesis — Malignant progression — Lung adenocarcinoma

## Introduction

Lung cancer holds the foremost position among the causes of cancer-related deaths, presenting a grave risk to human well-being (Nasim et al. 2019; Mederos et al. 2020; Lee and Kazerooni 2022; Rajendra et al. 2023; Yue et al. 2024; Asmat et al. 2024). From a histopathological perspective, the two primary categories of lung cancer are non-small cell lung cancer (NSCLC) and small cell lung cancer (SCLC) (Collins et al. 2007; Bade and Dela Cruz 2020; Abu Rous et al. 2023). NSCLC additionally includes lung adenocarcinoma (LUAD), squamous cell lung cancer (LUSC), and large cell lung carcinoma (LCC) (Collins et al. 2007; Bade and Dela Cruz 2020; Abu Rous et al. 2023). In lung cancer that originates in the lungs, LUAD has become the most common histological type, accounting for a large portion of cases, and its relative frequency of occurrence is continuously increasing (Vazquez et al. 2009; Wei et al. 2023; Li et al. 2023; Zhang et al. 2024). Despite the variety of current treatments for LUAD, including surgery, radiotherapy, targeted therapies, and combination therapies, although recent studies have shown that PCM1 is a promising prognostic biomarker, the prognosis and five-year survival rate for LUAD remain low due to the advanced stage and high heterogeneity of the majority of LUAD cases at the time of diagnosis (Guo et al. 2023; Zhang H et al. 2023). Therefore, it is essential to investigate the underlying mechanisms of LUAD and seek out novel therapeutic targets.

The alteration in metabolic pathways within tumor cells is pivotal in bolstering biosynthetic processes and protective

**Electronic supplementary material.** The online version of this article (doi: 10.4149/gpb_2025036) contains Supplementary material.

**Correspondence to:** Jing Li, Respiratory Medicine Center, Weifang People's Hospital, No. 151, Guangwen Street, Kuiwen District, Weifang 261000, China
E-mail: syc241028@163.com

© The Authors 2026. This is an **open access** article under the terms of the Creative Commons Attribution-NonCommercial 4.0 International License (https://creativecommons.org/licenses/by-nc/4.0/), which permits non-commercial use, distribution, and reproduction in any medium, provided the original work is properly cited.

antioxidant mechanisms (Du et al. 2013). Fatty acid metabolism reprogramming has been acknowledged as a distinctive feature of malignant tumors (Zhang L et al. 2023). The solute carrier family 25 member 1 (SLC25A1) plays a crucial role in the mitochondrial citrate cycle as a citrate carrier, participating in cell metabolic regulation, energy balance, fatty acid oxidation, and among other biological processes, and its genetic variations are associated with various diseases, making it as an important target for clinical research and drug development (Mosaoa et al. 2021; You et al. 2023; Zhang R et al. 2023). In colorectal cancer (CRC), SLC25A1 was highly expressed, driving CRC cell proliferation and colony formation by promoting fatty acid synthesis and increasing oxidative phosphorylation (OXPHOS), while inhibiting cell apoptosis (Yang et al. 2021). SLC25A1 was highly expressed in the metastatic sites of NSCLC, facilitating the emergence of therapeutic resistance and stemness traits by stimulating mitochondrial metabolism (Fernandez et al. 2018). In LUAD, the elevated expression of SLC25A1 was closely linked to poor prognosis and positively correlated with MSI, TMB, and CD276, and its knockdown demonstrated inhibitory effects in most cancer cell lines, significantly reducing the proliferation of LUAD cells (You et al. 2023). Given its ability to regulate cancer cell energy metabolism, SLC25A1 is considered a novel therapeutic target for cancer, yet the mechanism and role in LUAD energy metabolism remain incompletely understood and warrant further investigation.

The results of prior predictions indicated that targeted binding sites existed between Zinc finger protein 801 (MAZ) and the SLC25A1 promoter. Previous studies have confirmed that MAZ is highly expressed in lung cancer tissues and plays a role in promoting cancer progression (Wang et al. 2023; Chen et al. 2024). Meanwhile, preliminary experimental data demonstrated that knocking down MAZ could significantly inhibit the expression of SLC25A1 in lung cancer cells. Based on these findings, this study further explores the potential role and underlying mechanism of MAZ in LUAD. MAZ is a zinc finger protein that interacts with the homologue of the v-myc myelomatosis virus oncogene (c-Myc) (Zhang H et al. 2023). As an interaction partner of Myc protein, MAZ holds a significant position in modulating the processes of tumoral cell growth, metastasis, apoptosis, and autophagy, and is consequently regarded as an oncogene (Zheng et al. 2022; Darbellay et al. 2022; Lai et al. 2023; Wang et al. 2024). In triple-negative breast cancer, MAZ-induced upregulation of branched-chain α-keto acid dehydrogenase kinase (BCKDK) altered glucose utilization patterns and stimulated cellular proliferation by regulating the stability of glucose-6-phosphate dehydrogenase (Li et al. 2024). The MAZ transcription factor, acting as a subsequent target of the Cyr61/CCN1, facilitated the epithelial-mesenchymal transition and motility of pancreatic cancer cells through the CRAF-MAPK signaling cascade and augmented the stem cell-like properties (Maity et al. 2018). MAZ, as an upstream regulator of NEIL3, was highly expressed in LUAD tissues and targeted NEIL3 to inhibit DNA damage, thereby promoting cisplatin resistance and facilitating cell migration and invasion in LUAD (Wang et al. 2023).

The main focus of this study is to deeply explore the roles of MAZ and SLC25A1 in fatty acid synthesis and tumor growth processes in LUAD, with the goal of providing novel insights that can further promote the development of targeted therapeutic approaches for LUAD treatment.

## Materials and Methods

### *Bioinformatics analysis*

The level of SLC25A1 and MAZ in LUAD was predicted by the The Cancer Genome Atlas (TCGA) database (https://ualcan.path.uab.edu/analysis.html) and the UALCAN Clinical Proteomic Tumor Analysis Consortium (CPTAC) database (https://ualcan.path.uab.edu/analysis-prot.html). The Kaplan-Meier plotter (KM-plotter) (https://www.kmplot.com/analysis/) was utilized to assess the association between the levels of SLC25A1 and MAZ, as well as the clinical outcomes for LUAD patients. The genes associated with SLC25A1 in LUAD from the TCGA database, as well as the correlation between MAZ and SLC25A1 expression, were screened using the LinkedOmics (https://www.linkedomics.org/#/). Employing the hTF-target database (http://bioinfo.life.hust.edu.cn/hTFtarget#!/target), the potential transcription factors targeting SLC25A1 were predicted. The potential binding site between the promoter region of SLC25A1 and the transcription factor MAZ was predicted by the JASPAR database (https://jaspar.elixir.no/).

### *Sample collection*

Sixty-five pairs of LUAD tissue samples and the adjacent normal lung tissues were obtained. All patients with LUAD were first-time diagnosed and had not undergone any form of treatment before the operation. The specific inclusion criteria for patients with LUAD were detailed in Table 1. This study strictly adhered to international ethical guidelines in conducting human experiments. For the human research segment: all participants provided written informed consent, the study protocol was approved by the Medical Ethics Committee of Weifang People's Hospital, and all procedures complied with the principles outlined in the Declaration of Helsinki.

### *Cell culture*

Human LUAD cell lines, including A549, H1299, H1975, and PC9, as well as human bronchial epithelioid cells (16HBE),

purchased from Pricella (Wuhan, China), were grown in RPMI 1640 medium enriched with 10% fetal bovine serum (Proteintech, Wuhan, China) and containing penicillin and streptomycin (Proteintech).

*Plasmid construction and transfection*

The short hairpin RNA (shRNA) targeting SLC25A1 (shSLC25A1) or MAZ (shMAZ), non-targeting shRNA serving as the negative control (shControl), SLC25A1 overexpression vector (oeSLC25A1), and the blank vector serving as the blank control (oeNC) were acquired from Sangon Biotech (Shanghai, China). The introduction of plasmids into LUAD cells was achieved *via* Lipofectamine 3000 (Invitrogen, Waltham, MA, USA).

*RNA isolation and quantitative real-time RT-PCR (qRT-PCR)*

The extraction of total RNA from tissue samples (LUAD and adjacent normal lung tissues) and cell lines (H1975 and PC9) was accomplished with the aid of the TRIzol™ Plus RNA Purification Kit (Invitrogen). Following this, reverse transcription and qPCR were carried out in accordance with the guidelines furnished by the SuperScript™ III Platinum™ One-Step qRT-PCR Kit (Invitrogen). The primer sequences employed during the test were listed below: SLC25A1, forward 5'-CCGTCAGGTTTGGAATGTTCG-3' and reverse 5'-TAACCCCGTGGAAGAATCCTC-3'; MAZ, forward 5'-GACACGAGGAGAAAGTGCCA-3' and reverse 5'-CCTCACCAGTACCTTTGTTGC-3'; β-actin, forward 5'-CTTCGCGGGCGACGAT-3' and reverse 5'-CCACATAGGAATCCTTCTGACC-3'.

*Western blot analysis*

The isolation of total protein from tissue samples (LUAD and adjacent normal lung tissues) and cell lines (16HBE, A549, H1299, H1975, and PC9) was achieved with the aid of RIPA lysis buffer and extraction buffer (Invitrogen), which contained Halt™ protease inhibitor cocktail (Invitrogen). The proteins in the samples underwent separation through SDS-polyacrylamide gel electrophoresis, and they were then transferred to the polyvinylidene fluoride (PVDF) membrane. Then, the membranes were sealed with Western blot rapid sealing solution (Proteintech). After the sealing process, the membrane underwent incubation with the anti-SLC25A1 (15235-1-AP, 1:3000, Proteintech), anti-MAZ (ab85725, 1:5000, Abcam, Cambridge, UK), or anti-β-actin (20536-1-AP, 1:5000, Proteintech) antibodies at a temperature of 4°C for a duration of one night. After the primary antibody had been allowed to bind, the secondary antibody (SA00001-2, 1:8000, Proteintech) was introduced and allowed to react at 37°C for 1 h. The results were finally visualized using a sensitive ECL chemiluminescent detection kit (Proteintech).

**Table 1.** The clinicopathologic features in LUAD patients

| Parameter | *n* |
|---|---|
| Age, years | |
| <60 | 29 |
| ≥60 | 36 |
| Sex | |
| Male | 48 |
| Female | 17 |
| Smoking history | |
| Yes | 42 |
| No | 23 |
| Tumor location | |
| Left lobe | 31 |
| Right lobe | 34 |
| Tumor size | |
| <3 | 30 |
| ≥3 | 35 |
| TNM stage | |
| <III stage | 47 |
| ≥III stage | 18 |
| Lymph node metastasis | |
| No | 41 |
| Yes | 24 |

*Cell counting kit-8 (CCK8) assay*

The 96-well plate, with each well containing 100 μl of cell suspension, was placed in an environment of 37°C and 5% $CO_2$ and was maintained in incubation for 24 h. Afterwards, the medium was discarded, and fresh medium incorporating CCK8 solution (Beyotime, Shanghai, China) was introduced. After that, the samples underwent incubation for 2 h at 37°C in a 5% $CO_2$ incubator. Finally, the absorbance of each well underwent measurement by an enzyme labeling apparatus.

*Cell proliferation assay*

The VF 488 Click-iT EdU universal cell proliferation assay kit (MedChemExpress, Shanghai, China) was employed for assessing cell proliferation. In brief, the logarithmically growing cells were planted in a 96-well plate and nurtured in the full growth medium supplemented with 50 μM 5-ethynyl-2'-deoxyuridine for 2 h. Afterwards, the medium was removed, and the cells were immobilized using 50 μl of cell fixation solution at 37°C for 30 min Subsequently, they were treated with 50 μl of 2 mg/ml glycine solution at 37°C for 5 min. After that, 100 μl of a permeabilization solution was introduced,

followed by an additional 10 min. of incubation. Then, 100 µl of Click-iT working solution was evenly added to cover the cells, and they were kept in the dark at 37°C for a period of 30 min. to undergo incubation. Ultimately, the cells were analyzed using fluorescence microscopy.

*Colony-formation assay*

The logarithmically growing cells were digested and dispersed to form a monomeric cell suspension in medium. They were subsequently planted in culture dishes and allowed to incubate at 37°C in an incubator with 5% $CO_2$. When visible clones were formed in the dishes, the incubation was terminated. After discarding the medium, the cells underwent fixation with methanol for 15 min. After removal of the fixative, they were colored with a 0.5% solution of crystal violet for 20 min. Finally, the staining solution was washed off, and the clone count was determined under a microscope.

*Flow cytometry*

Cells in the logarithmic growth phase were gathered, treated with trypsin to disintegrate them, and subsequently dispersed into a suspension of individual cells. The cell suspension was transferred into a centrifuge tube and centrifuged at 2000 revolutions *per* minute for duration of 5 min, followed by the discarding of the supernatant. The cellular specimens were then rinsed using phosphate-buffered saline (PBS) and centrifuged in a centrifuge, and the resultant supernatant was discarded. Next, the cellular specimens were re-dispersed in 1×Binding Buffer; subsequently, 5 µl of Annexin V-FITC-A (Elabscience, Wuhan, China) and 5 µl of PI-PE-A (Elabscience) were added, and then allowed to sit at 37°C for 15 min. while being protected from light. Ultimately, apoptosis was ascertained through flow cytometry (Thermo Fisher Scientific).

*Determination of neutral lipid content*

The LUAD cells (H1975 and PC9) in the logarithmic growth phase were subjected to trypsin digestion and collected. Subsequently, they were inoculated into cell culture dishes to ensure they maintained good growth conditions. Then, the cells were fixed using formaldehyde solution (Beyotime) and permeabilized with 0.1% Triton X-100 (Beyotime) for 5 min. Afterward, 1 µM BODIPY493/503 (MedChemExpress) was added to the cell samples and incubated at 37°C in the dark for 30 min to ensure sufficient binding of the BODIPY493/503 dye to the neutral lipids within the cells. Following washing, the cell culture dishes were sealed with anti-fluorescence quench sealing tablets (Invitrogen). Finally, the stained cells were observed under a fluorescence microscope, and the content of neutral lipids within the cells was assessed based on the distribution of fluorescence intensity.

*Determination of intracellular lipid compounds*

The contents of free fatty acids, triglycerides, phospholipids, and cholesterol within the cells were determined using the Free Fatty Acids (NEFA/FFA) Colorimetric Assay Kit (Elabscience), the Triglyceride (TG) Colorimetric Assay Kit (Elabscience), the Phospholipid Quantitative Detection Kit (Merck, Darmstadt, Germany), and the Free Cholesterol (FC) Colorimetric Assay Kit (Elabscience), respectively, all in accordance with the instructions provided.

*Luciferase reporter assay*

The luciferase reporter gene plasmid containing the SLC25A1 promoter and the renilla luciferase internal control plasmid were designed by Gene Create (Wuhan, China). The luciferase reporter gene plasmid, the renilla luciferase internal control plasmid, along with either the shMAZ or shControl plasmid, were introduced simultaneously into H1975 or PC9 cells using Lipofectamine 3000 (Invitrogen). After the cells were transfected, they were further cultured under appropriate conditions for 48 h. Subsequently, the cells were collected and lysed, and the luciferase substrate and Renilla luciferase substrate (Invitrogen) were added to the lysates, respectively, followed by incubation in dim conditions for 30 min. Finally, the luminescence intensity was measured using a fluorometer, and the ratio of luciferase to renilla luciferase luminescence intensity was calculated accordingly.

*Chromatin immunoprecipitation (ChIP) assays*

ChIP assays were conducted utilizing the Pierce™ Magnetic ChIP Kit (Invitrogen). Specifically, chromatin was broken down by sonication after cross-linking and crushing of H1975 and PC9 cells. Anti-SLC25A1 (15235-1-AP, 1:300, Proteintech) or anti-IgG (30000-0-AP, 1:300, Proteintech) antibodies were added to chromatin and left to incubate for an entire night at 4°C. After incubation, Protein A/G magnetic beads were introduced to continue the incubation process for 2 h. Then, the beads underwent washing in lysis buffer, subsequently undergoing Western blot analysis.

*Cancer cell xenograft model in vivo*

BALB/c nude mice, aged four weeks, were obtained from Beijing Vital River Laboratory Animal Technology Co., Ltd. (Beijing, China). A total of eight mice were assigned to each experimental group, and each experiment was replicated three times independently. For xenograft models, $5\times10^6$

H1975 cells from the shControl or shMAZ groups were subcutaneously injected into the right flank of mice. Seven days of post-transplantation, tumor growth was monitored every seven days. The tumors were surgically excised five weeks later to evaluate the expression levels of MAZ and SLC25A1 *via* immunohistochemistry (IHC). This study strictly adhered to international ethical guidelines in conducting animal experiments. The experimental design followed the "3Rs principle" (Replacement, Reduction, Refinement), with all procedures authorized by the Animal Ethics Committee of Weifang People's Hospital and conducted in compliance with the National Institutes of Health (NIH) Guide for the Care and Use of Laboratory Animals.

*IHC*

The tissues of mice were fixed, dehydrated, paraffin-embedded, and sliced, and then blocked with 5% bovine serum albumin (BSA) at 37°C for 1 h. After that, the sections were treated with anti-SLC25A1 (15235-1-AP, 1:100, Proteintech) or anti-MAZ (ab85725, 1:1000, Abcam) antibodies at 37°C for 1 h. After the completion of the primary antibody incubation, the sections underwent treatment with the secondary antibody (RGAR011, 1:4000, Proteintech) for 30 min at 37°C. Subsequently, DAB chromogenic solution (Solarbio, Beijing, China) was introduced and permitted to incubate for 5 min in a light-shielded environment. Following washing, Mayer's hematoxylin (Solarbio) was applied for 2 min, and the section slices were sealed with neutral gum (Solarbio) for microscopic observation.

*Statistical analysis*

The experimental data were displayed as mean ± standard deviation (SD), with three biological replicates included for each experimental condition, and were analyzed utilizing GraphPad Prism 7.0 statistical software (GraphPad Software, Boston, MA, USA). Statistical comparisons between groups were performed using Student's *t*-test (for two-group comparisons) and one-way analysis of variance (ANOVA) (for multiple-group comparisons). A $p$ value of less than 0.05 was deemed to be statistically significant.

## Results

*SLC25A1 is upregulated in LUAD and is associated with a poor prognosis*

To determine the expression level of SLC25A1 in LUAD tissues, we analyzed the TCGA and CPTAC databases, revealing that SLC25A1 was highly expressed in LUAD (Fig. 1A,B). The overall survival (OS) for patients exhibiting high expression of SLC25A1 was notably shorter than those with low expression of the same gene. Similarly, the first progression (FP) of the patients with elevated expression of SLC25A1 was notably shorter in comparison to those with low expression of SLC25A1 (Fig. 1C). Simultaneously, the qRT-PCR and Western blot results showed that the expression level of SLC25A1 was significantly increased in LUAD tissues (Fig. 1D,E). Correspondingly, a notable rise in SLC25A1 was detected in the LUAD cell lines (A549, H1299, H1975, and PC9) in comparison to human bronchial epithelioid cell 16HBE (Fig. 1F). Overall, these findings indicate that SLC25A1 exhibits the high expression in LUAD and is closely associated with poor prognosis in patients.

*SLC25A1 promotes LUAD cell proliferation and inhibits apoptosis*

H1975 and PC9 cells were transfected with shSLC25A1 or shControl to verify the role of SLC25A1 on LUAD cells. The Western blot results indicated that SLC25A1 expression was successfully decreased in LUAD cells by transfection of shSLC25A1 (Fig. 2A). Subsequently, CCK-8, EdU, and colony formation assays revealed that SLC25A1 knockdown significantly hindered cell viability, proliferation, and colony formation in H1975 and PC9 cells (Fig. 2B–D). Flow cytometry analysis further revealed an elevation in the rate of cell apoptosis in H1975 and PC9 cells after the knockdown of SLC25A1 (Fig. 2E,F). In summary, SLC25A1 enhances the viability and proliferation of H1975 and PC9 cells while inhibiting apoptosis.

*SLC25A1 promotes fatty acid synthesis in LUAD cells*

To clarify the mechanism which SLC25A1 affects in LUAD cells, we assessed the effects of SLC25A1 knockdown on the lipid levels within these cells. Staining of cells with the fluorescent lipophilic dye BODIPY 493/503, we found that the knockdown of SLC25A1 significantly decreased the amount of neutral lipids in H1975 and PC9 cells (Fig. 3A). Furthermore, when SLC25A1 was knocked down, the reduction of intracellular levels of free fatty acids, triglycerides, phospholipids, and cholesterol in H1975 and PC9 cells was observed (Fig. 3B–E). To sum up, SLC25A1 facilitates the synthesis of neutral lipids, free fatty acids, triglycerides, phospholipids, and cholesterol in H1975 and PC9 cells.

*MAZ is overexpressed in LUAD and is positively correlated with SLC25A1*

To further investigate the mechanism of SLC25A1 in lipid metabolism in LUAD, we utilized the linkedOmics database to screen for genes associated with SLC25A1 in LUAD (Fig. 4A). We identified 144 transcription factors that potentially

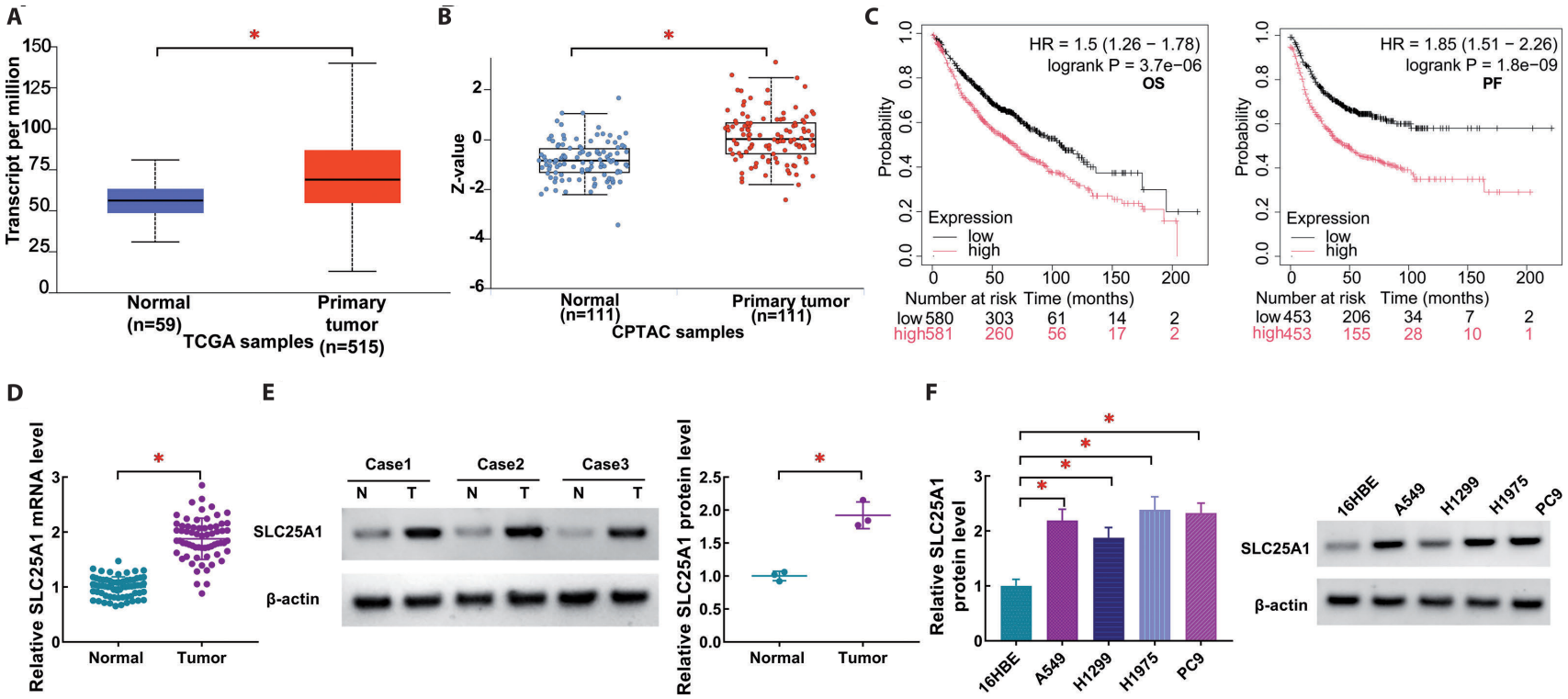



**Figure 1.** SLC25A1 expression is elevated in LUAD and is linked to unfavorable prognosis. **A.** SLC25A1 levels in LUAD were analyzed based on TCGA database. **B.** The expression of SLC25A1 in LUAD was analyzed based on the CPTAC database. **C.** The KM-plotter database was used to analyze OS (left panel) and FP (right panel) in patients with LUAD. **D.** The levels of SLC25A1 in patient samples of LUAD and the adjacent normal tissues were determined by qRT-PCR. **E.** Western blot assay was performed to measure the levels of SLC25A1 in both LUAD tissues and the adjacent normal counterparts. **F.** Western blot analysis was conducted to determine the levels of SLC25A1 in LUAD cells, as well as in normal human bronchial epithelioid cells. * $p < 0.05$.

target SLC25A1 using the hTF-target database. Subsequently, we interacted these transcription factors with 531 genes positively correlated with SLC25A1, and ultimately screened out three common factors: MAZ, HSF1, and GMEB2 (Fig. 4B). The qRT-PCR assay results demonstrated that when HSF1 and GMEB2 were knocked down, there were no significant changes in the expression of SLC25A1; however, after knocking down MAZ, the expression level of SLC25A1 showed a significant decline (Fig. S1 in Supplementary material). MAZ was upregulated in lung cancer and had a cancer-promoting effect, so it was selected for subsequent research (Chen et al. 2024). Both TCGA and CPTAC databases indicated that MAZ was upregulated in LUAD (Fig. 4C,D). Kaplan-Meier survival analysis revealed that LUAD patients with high expression of MAZ had shorter OS and poorer FP compared to those with low expression of MAZ (Fig. 4E). LinkedOmics database indicated that there was a positive correlation between the expression of MAZ and SLC25A1 in LUAD tissues (Fig. 4F). Furthermore, qRT-PCR analysis of LUAD tissues validated a significant increase

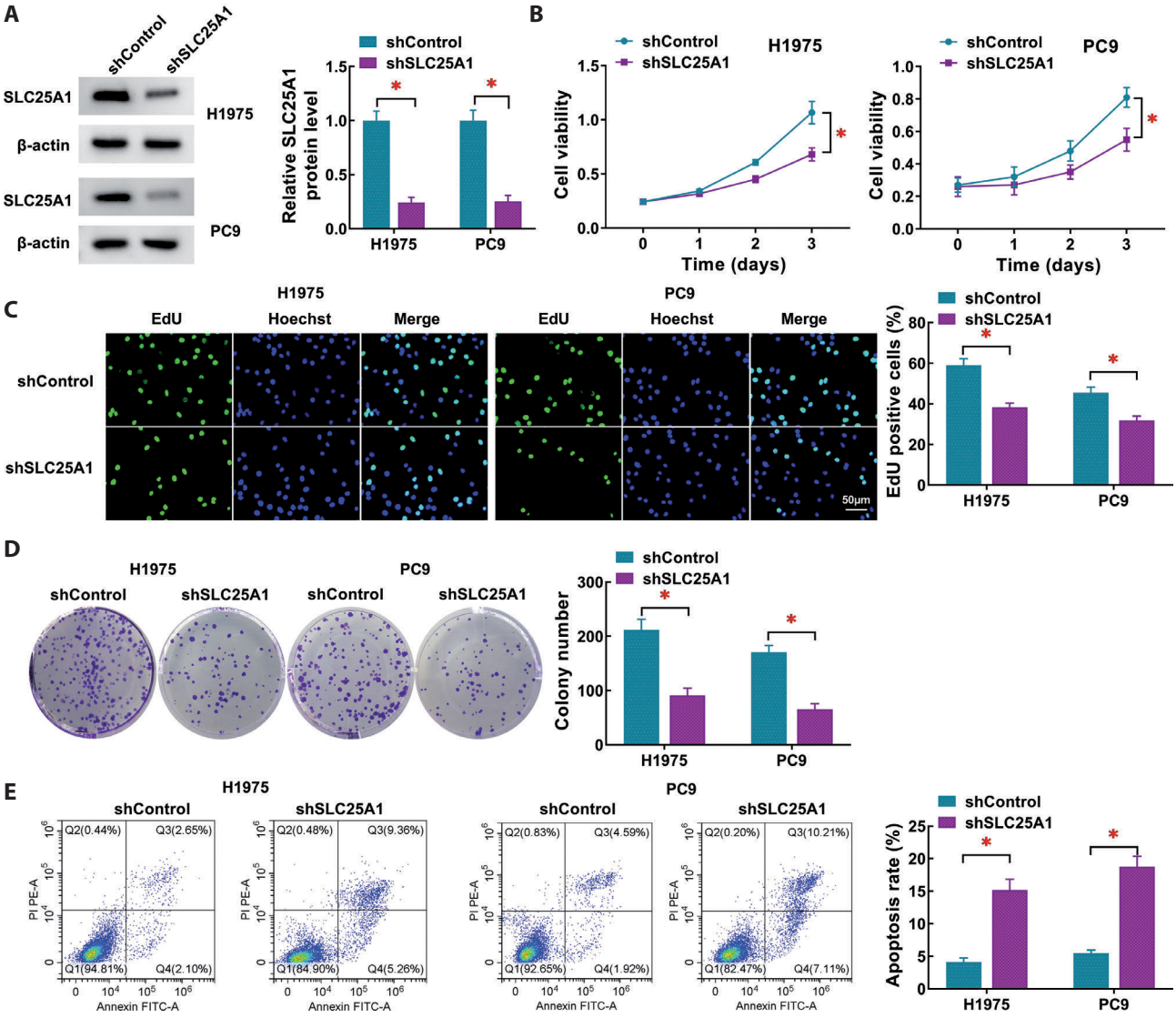



**Figure 2.** SLC25A1 stimulates the proliferation of LUAD cells while suppressing the apoptosis. H1975 and PC9 cells were divided into shControl and shSLC25A1 groups, and each group was transfected with the corresponding plasmids. **A.** Western blot analysis was performed to assess the transfection efficiency in H1975 and PC9 cells after SLC25A1 knockdown. **B.** CCK8 assays were conducted to detect the cell viability of H1975 and PC9 cells. **C.** Cell proliferation ability of H1975 and PC9 cells was measured by EdU assay. **D.** Colony-formation assay was conducted to examine the colony-formation ability of H1975 and PC9 cells. **E.** Flow cytometry revealed the apoptosis of A549 and H1299 cells. * $p < 0.05$.

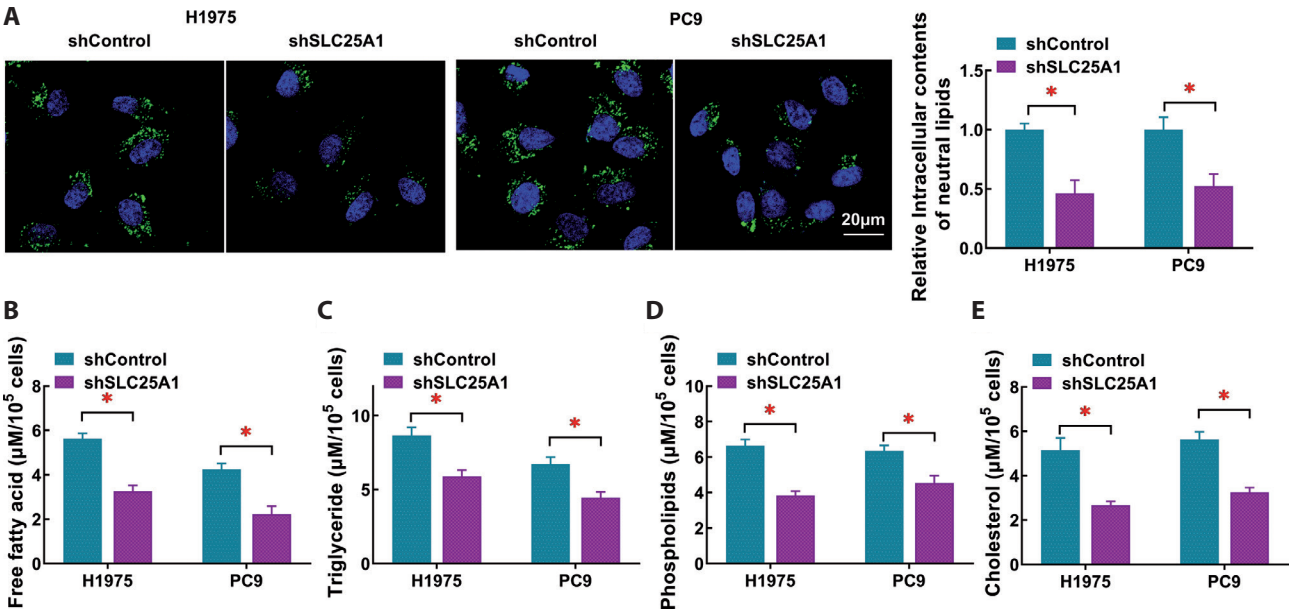



**Figure 3.** SLC25A1 enhances the production of fatty acids in LUAD cells. H1975 and PC9 cells were divided into shControl and shSLC25A1 groups, and each group was transfected with the corresponding plasmids. **A.** H1975 and PC9 cells were stained with BODIPY 493/503 to visualize neutral lipids. **B.** The concentrations of free fatty acids were quantified in H1975 and PC9 cells using a specific kit. **C.** The levels of triglycerides were measured in H1975 and PC9 cells with the use of a dedicated kit. **D.** H1975 and PC9 cells were assayed for the phospholipid levels utilizing a specific kit. **E.** Cholesterol levels in H1975 and PC9 cells were determined using a specific kit. * $p < 0.05$.

in MAZ levels (Fig. 4G), which positively correlated with SLC25A1 expression (Fig. 4H). The results of the Western blot indicated that, compared to normal tissues and cells (16HBE), MAZ exhibited a relatively high expression in LUAD tissues and cells (H1975 and PC9) (Fig. 4I,J). The aforementioned results indicate that MAZ is overexpressed in LUAD and is closely associated with poor prognosis in LUAD patients, and its expression level is positively correlates with SLC25A1.

*Transcription factor MAZ has a targeted regulatory relationship with SLC25A1*

To explore the regulatory mechanism of MAZ in LUAD progression, we employed the JASPAR database to analyze the transcription factor MAZ and discovered two binding sites (BS1 and BS2) located within the promoter region of SLC25A1 (Fig. 5A). The aforementioned prediction was further corroborated through luciferase reporter assay and ChIP. The outcomes demonstrated an interaction between MAZ and the SLC25A1 promoter (Fig. 5B–D). The results of qRT-PCR and Western blot assays showed that the expression of SLC25A1 was significantly reduced in the shMAZ group compared to the control group (Fig. 5E,F). In summary, these discoveries suggest that MAZ serves as the upstream regulatory factor of SLC25A1 and has the ability to directly enhance the transcription of SLC25A1.

*MAZ promotes malignant behaviors of LUAD cells via SLC25A1*

To further investigate the function of the MAZ/SLC25A1 axis in the malignant progression of LUAD. We established the following experimental groups: shControl+oeNC, shMAZ+oeNC, and shMAZ+oeSLC25A1. The results showed that there was a significant reduction in SLC25A1 expression in the shMAZ+oeNC group when compared to the control group, whereas it was restored in the shMAZ+oeSLC25A1 group (Fig. 6A). Next, we evaluated LUAD cell viability, proliferation, and colony formation. The results revealed that these parameters were suppressed in the shMAZ+oeNC group, but they were rescued in the shMAZ+oeSLC25A1 group (Fig. 6B–D). Meanwhile, cell apoptosis was detected by flow cytometry. The results illuminated that compared to the control group; there was a significant increase in cell apoptosis in the shMAZ+oeNC group, whereas this effect was mitigated in the shMAZ+oeSLC25A1 group (Fig. 6E). In addition, knockdown of MAZ significantly reduced neutral lipid content in H1975 and PC9 cells, which was reversed by the overexpression of SLC25A1 (Fig. 6F). When MAZ expression was reduced, the levels of free fatty acids, triglycerides, phospholipids, and cholesterol in H1975 and PC9 cells all decreased significantly, while overexpressing SLC25A1 mitigated these decrease (Fig. 6G–J). The findings indicate that MAZ facilitates the malignant

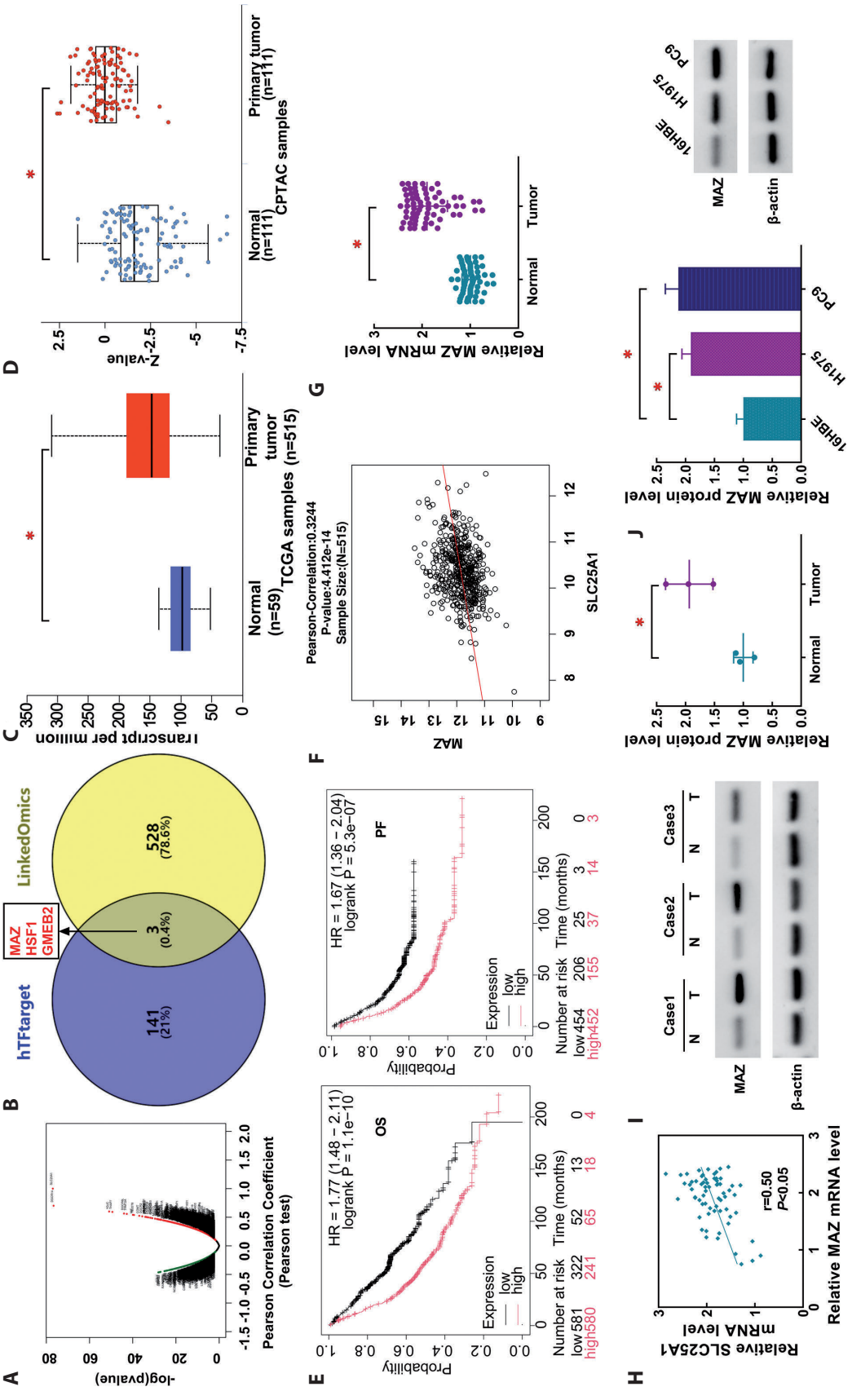



**Figure 4.** MAZ expression in LUAD is positively correlated with SLC25A1 levels. **A.** Volcano map of genes related to SLC25A1 in LUAD was screened using the LinkedOmics database. **B.** Venn diagram displayed the intersection of genes positively correlated with SLC25A1 in LUAD and potential SLC25A1-targeting transcription factors predicted by hTFtarget database. **C.** The levels of MAZ in LUAD tissues were examined utilizing the TCGA database. **D.** MAZ levels in LUAD tissues were analyzed based on the CPTAC database. **E.** The KM-plotter database was employed to assess OS (left panel) and FP (right panel) in LUAD patients. **F.** The LinkedOmics database provided a prediction of the correlation between MAZ and SLC25A1 in LUAD tissues. **G.** qRT-PCR was utilized to measure the levels of MAZ in LUAD tissues. **H.** Pearson correlation analysis of MAZ and SLC25A1. **I.** Western blot was implemented to detect the levels of MAZ in both LUAD tissues and the adjacent normal counterparts. **J.** The results of the Western blot assay showed the levels of MAZ in LUAD cells, as well as in normal human bronchial epithelioid cells. * $p < 0.05$.

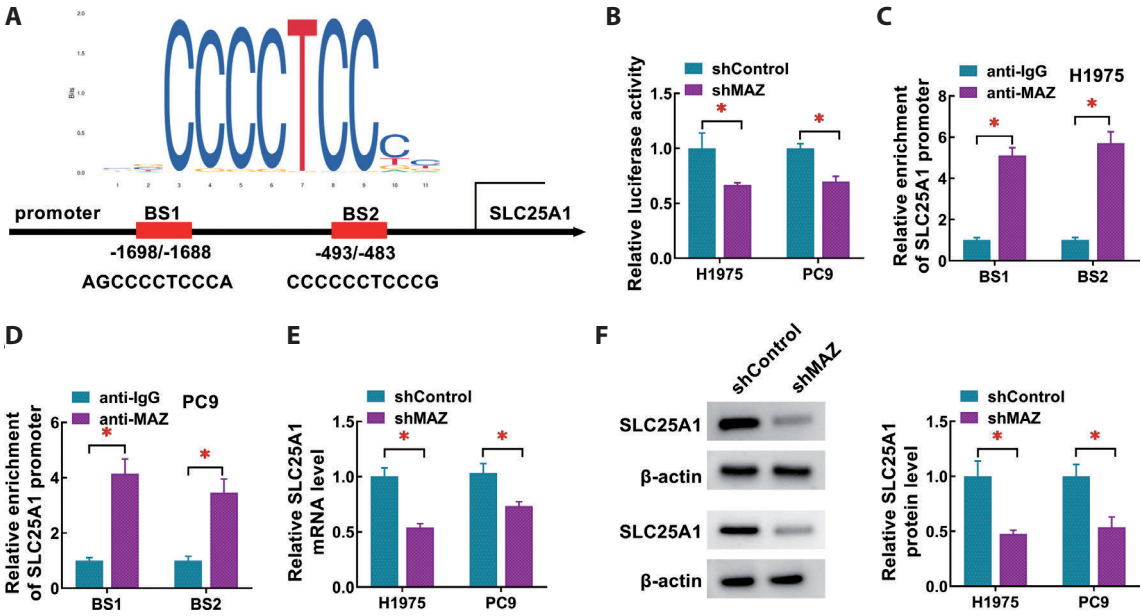



**Figure 5.** MAZ is an upstream regulatory molecule of SLC25A1. H1975 and PC9 cells were divided into shControl and shMAZ groups, and each group was transfected with the corresponding plasmids. **A.** JASPAR database was employed for predicting the binding sites of MAZ on the promoter region of SLC25A1. **B-D.** Luciferase reporter assay and ChIP were performed to verify the binding of MAZ to the SLC25A1 promoter region. **E,F.** qRT-PCR and Western blot were conducted to measure the expression level of SLC25A1 after MAZ knockdown. * $p < 0.05$.

progression of LUAD through the activation of SLC25A1 expression.

*MAZ promotes malignant progression of LUAD in vivo*

We subsequently assessed the effects of MAZ silencing on the malignant progression of LUAD *in vivo*. The results demonstrated that, compared to the shControl group, the tumors in the shMAZ group exhibited a significant reduction in both volume and weight (Fig. 7A–C). The levels of MAZ and SLC25A1 in the tumors were detected by IHC, and the results showed that in comparison to the shControl group, the levels of both MAZ and SLC25A1 were significantly reduced in the shMAZ group (Fig. 7D). These data suggest that silencing MAZ not only inhibits the malignant progression of LUAD *in vivo* but also effectively reduces SLC25A1 expression in LUAD tumors.

## Discussion

The abnormally regulated transcription factors have a crucial role in tumor development. Abnormal expression of the transcription factor MAZ was observed in primary liver cancer (PLC), prostate cancer (PCa), NSCLC, gastric cancer (GC), and basal-like breast cancer (BLBC) (Yu et al. 2017; Thommen et al. 2018; Wang et al. 2020; Wu et al. 2024; Xiao et al. 2024). In previous studies, MAZ has been shown to exert its oncogenic effects through various signaling pathways. For instance, MAZ activates the mitogen-activated protein kinase (MAPK) signaling pathway by facilitating transcriptional reprogramming, thereby promoting the progression of thyroid cancer (TC) (Zeng et al. 2024). In PCa, MAZ is upregulated in bone metastasis tissues and facilitates PCa cell bone metastasis *via* the transcriptional activation of RAS signaling and V-ki-ras2 kirsten ratsarcoma viral oncogene homolog (KRAS)-mediated Ral guanine nucleotide exchange factors (RalGEFs) signaling (Yang et al. 2019). In our current research, we had identified that the transcription factor MAZ possessed the capability to augment the malignant proliferation of LUAD, both in vitro and *in vivo*. Consistent with this observation, MAZ expression in LUAD samples exhibited the elevated levels compared to healthy tissues, and this elevation strongly correlated with patient prognosis. However, the specific molecular mechanisms underlying MAZ-mediated LUAD progression, especially its interaction with key downstream molecules, remain to be fully elucidated.

SLC25A1 functions as a transporter of mitochondrial citrate and holds a central position in cellular energy metabolism by sustaining mitochondrial citrate reserves and redox balance while also engaging in the oxidative phos-

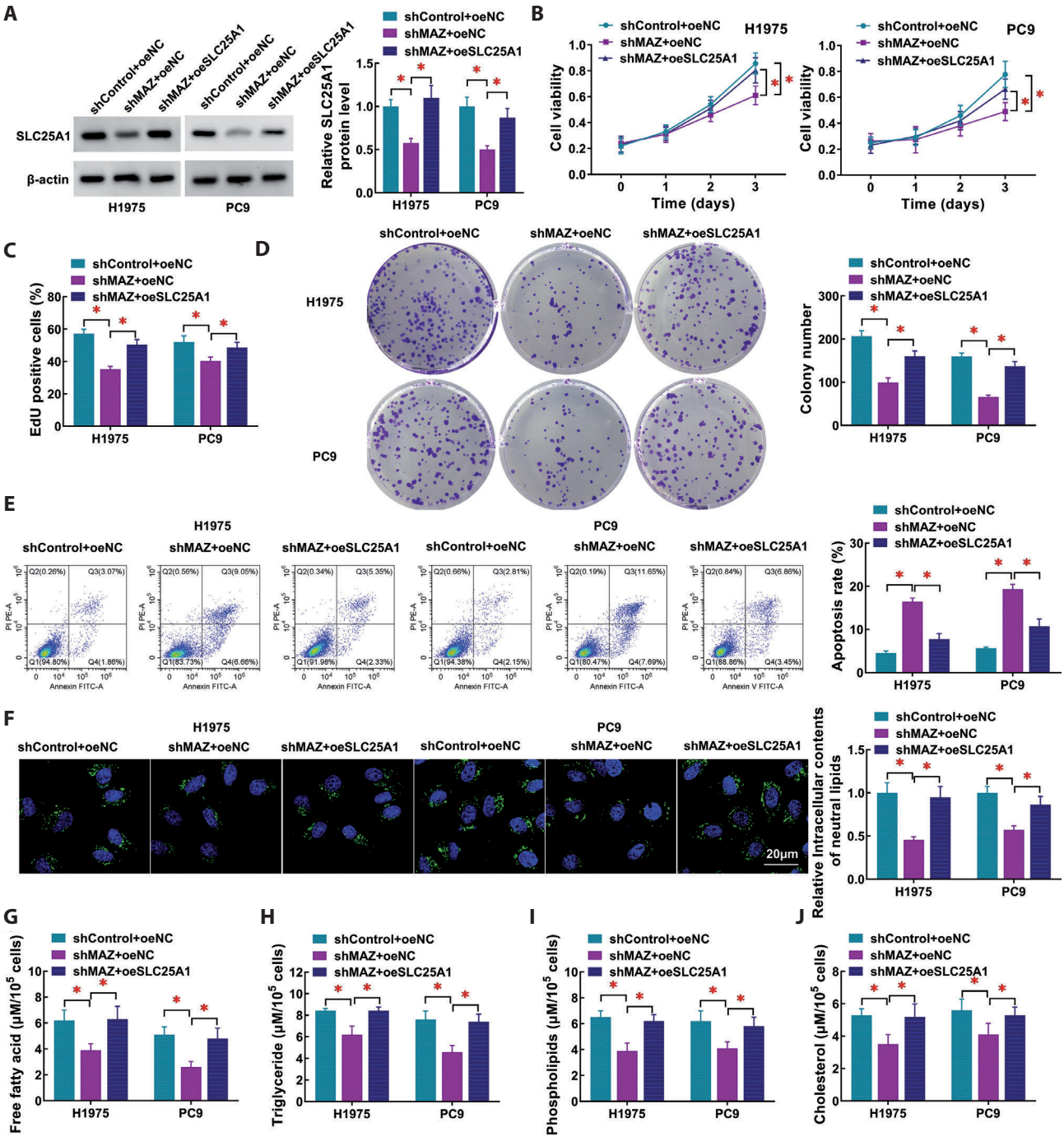



**Figure 6.** MAZ drives the malignant behaviors of LUAD cells by regulating SLC25A1. H1975 and PC9 cells were divided into shControl+oeNC group, shMAZ+oeNC group and shMAZ+oeSLC25A1 group, and each group was transfected with the corresponding plasmids. **A.** SLC25A1 expression in H1975 and PC9 cells was detected by Western blot. **B.** The viability of H1975 and PC9 cells was determined using CCK8 assay. **C.** EdU assay was performed to measure the cell proliferation of H1975 and PC9 cells. **D.** The colony-formation ability of H1975 and PC9 cells was measured by colony-formation assay. **E.** The apoptosis of H1975 and PC9 cells was assessed using flow cytometry. **F.** H1975 and PC9 cells were stained with BODIPY 493/503 to visualize neutral lipids. **G.** The concentrations of free fatty acids were quantified in H1975 and PC9 cells using specific colorimetric assay kit. **H.** The levels of triglycerides were measured in H1975 and PC9 cells with the use of specific colorimetric assay kit. **I.** H1975 and PC9 cells were assayed for the phospholipid levels utilizing Quantitative Detection Kit. **J.** Cholesterol levels in H1975 and PC9 cells were determined using specific colorimetric assay kit. * $p < 0.05$.

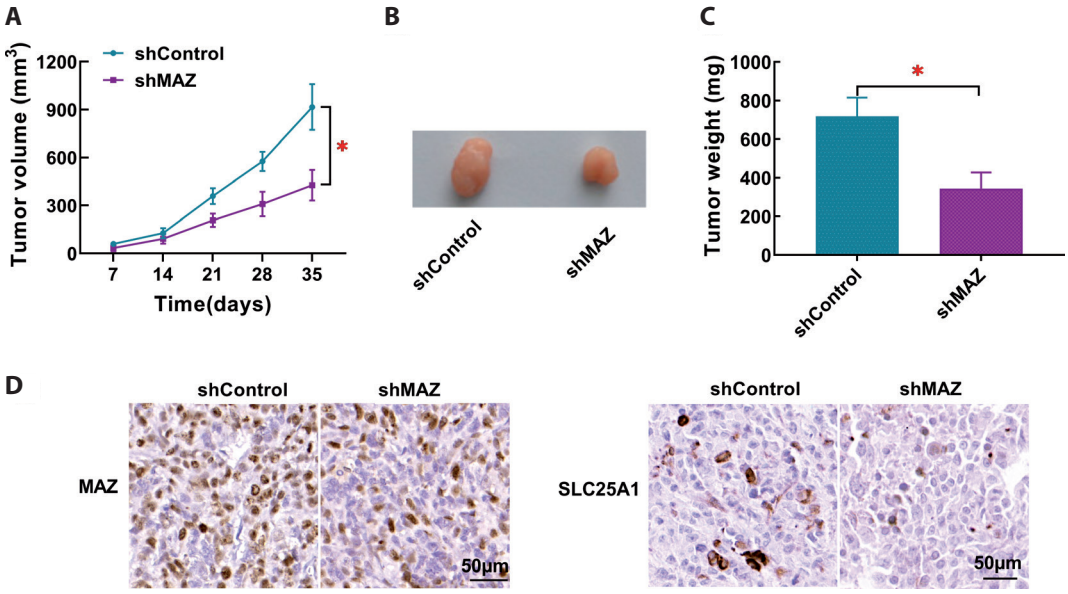



**Figure 7.** *In vivo* verification of the inhibitory effect of silencing MAZ on malignant progression of LUAD. Mice were divided into shControl and shMAZ groups, and each group was injected subcutaneously with the corresponding cells. **A.** The growth curve of xenograft tumors. **B,C.** The weight of xenograft tumors. **D.** Detection of MAZ and SLC25A1 levels in xenograft tumors by IHC. * $p < 0.05$.

phorylation process, which constitutes the primary way for cells to produce adenosine triphosphate for energy (Liu et al. 2022; Yang et al. 2022; Zhang et al. 2025). Research indicated that SLC25A1 regulated the resistance of cancer cells to radiotherapy by maintaining cellular redox homeostasis and modulating mitochondrial metabolic activities (Hlouschek et al. 2018). In pancreatic cancer, KRASG12D stimulated the upregulation of SLC25A1 *via* GLI1, consequently elevating the levels of cytosolic citrate, fatty acid synthesis, and essential enzymes in lipid metabolism, thereby fostering tumorigenesis (Zhang R et al. 2023). This study demonstrates that SLC25A1 is abundantly expressed in LUAD, significantly promoting the synthesis of newly formed lipids. Consequently, it enhances the viability and proliferation of LUAD cells while inhibiting apoptosis. Regarding the MAZ-SLC25A1 signaling pathway in LUAD, this study provides clear evidence of their causal link. Bioinformatics analysis using linkedOmics and hTF-target databases revealed MAZ as a key transcription factor positively correlated with SLC25A1 expression. JASPAR database analysis predicted two MAZ binding sites in the SLC25A1 promoter, confirmed by luciferase reporter and ChIP assays, indicating direct regulation. qRT-PCR and Western blot results showed that MAZ knockdown reduced SLC25A1 expression, while overexpression increased it. Thus, MAZ acts as an upstream regulator, directly enhancing SLC25A1 transcription.

Mechanistically, MAZ facilitates fatty acid biosynthesis in LUAD cells by enhancing SLC25A1 expression through transcriptional activation. The increased expression of SLC25A1 leads to an elevation in the transport of mitochondrial citrate to the cytoplasm (Mosaoa et al. 2021). Citrate is a key precursor for fatty acid synthesis (Duarte Lau and Giugliano 2023). In the cytoplasm, citrate is converted to acetyl-CoA, which is then used for the synthesis of fatty acids, triglycerides, phospholipids, and cholesterol (Rajpurohit and Eiteman 2024). The enhanced fatty acid synthesis provides the necessary building blocks for cell membrane formation and energy storage, thereby promoting the viability and proliferation of LUAD cells (Samovski et al. 2023). At the same time, the altered lipid metabolism may also affect cell signaling pathways and the tumor microenvironment, further contributing to the malignant progression of LUAD (Bian et al. 2021).

This study demonstrates that in LUAD, the upregulation of SLC25A1 is associated with poor prognosis; moreover, it stimulates cell proliferation and inhibits cell apoptosis while also facilitating fatty acid synthesis. Additionally, the transcription factor MAZ, which is highly expressed in LUAD and exhibits a targeted regulatory relationship with SLC25A1. MAZ drives the malignant progression of LUAD by regulating SLC25A1. These results may offer a novel approach for targeted therapy in patients with LUAD. In future research, further exploration of the MAZ-SLC25A1 signaling pathway, such as identifying other downstream molecules and signaling cascades involved, and investigating the potential of targeting this pathway for therapeutic

intervention, will be of great significance for improving the treatment of LUAD.

**Data availability statement.** The data are available from the corresponding author on reasonable request.

**Conflict of interest.** The authors declare that they have no conflicts of interest.

**Funding.** This research was supported by the Youth General Program of the Shandong Provincial Department of Science and Technology (ZR2024QH550).

## References

Abu Rous F, Singhi EK, Sridhar A, Faisal MS, Desai A (2023): Lung cancer treatment advances in 2022. Cancer Invest **41,** 12-24 https://doi.org/10.1080/07357907.2022.2119479

Asmat U, Anum R, Mohammad YA, Serag Eldin IE, Farid M, Najeeb U, Somia S, Touseef N, Haroon I (2024): Sanguinarine attenuates lung cancer progression via oxidative stress-induced cell apoptosis. Curr. Mol. Pharmacol. **17,** 1-25 https://doi.org/10.2174/0118761429269383231119062233

Bade BC, Dela Cruz CS (2020): Lung Cancer 2020: Epidemiology, etiology, and prevention. Clin. Chest. Med. **41,** 1-24 https://doi.org/10.1016/j.ccm.2019.10.001

Bian X, Liu R, Meng Y, Xing D, Xu D, Lu Z (2021): Lipid metabolism and cancer. J. Exp. Med. **218,** e20201606 https://doi.org/10.1084/jem.20201606

Chen Y, Zhu X, Wang J, Hu J, Zhang J, Zhang X, Han L, Yu H, Hu H, Fei K et al. (2024): MAZ promotes tumor proliferation and immune evasion in lung adenocarcinoma. Oncogene **43,** 3619-3632 https://doi.org/10.1038/s41388-024-03194-y

Collins LG, Haines C, Perkel R, Enck RE (2007): Lung cancer: diagnosis and management. Am. Fam. Physician **75,** 56-63

Darbellay F, Rouco R, Andrey G (2022): MAZ regulates chromatin domain insulation and genome architecture. Nat. Genet. **54,** 96-97 https://doi.org/10.1038/s41588-021-00995-9

Du W, Jiang P, Mancuso A, Stonestrom A, Brewer MD, Minn AJ, Mak TW, Wu M, Yang X (2013): TAp73 enhances the pentose phosphate pathway and supports cell proliferation. Nat. Cell Biol. **15,** 991-1000 https://doi.org/10.1038/ncb2789

Duarte Lau F, Giugliano RP (2023): Adenosine triphosphate citrate lyase and fatty acid synthesis inhibition: A narrative review. JAMA Cardiol. **8,** 879-887 https://doi.org/10.1001/jamacardio.2023.2402

Fernandez HR, Gadre SM, Tan M, Graham GT, Mosaoa R, Ongkeko MS, Kim KA, Riggins RB, Parasido E, Petrini I, et al. (2018): The mitochondrial citrate carrier, SLC25A1, drives stemness and therapy resistance in non-small cell lung cancer. Cell. Death Differ. **25,** 1239-1258 https://doi.org/10.1038/s41418-018-0101-z

Guo ZH, Liang JH, Xin Z, Zhang X, Ai Q, Xie ZX, Zhao HN, Wu FY, Tan ZF, Yin WQ, et al (2023): PCM1: A potential prognostic biomarker correlated with immune infiltration in lung adenocarcinoma. Curr. Proteomics **20,** 208-221 https://doi.org/10.2174/0115701646270898231123065507

Hlouschek J, Hansel C, Jendrossek V, Matschke J (2018): The mitochondrial citrate carrier (SLC25A1) sustains redox homeostasis and mitochondrial metabolism supporting radioresistance of cancer cells with tolerance to cycling severe hypoxia. Front. Oncol. **8,** 170 https://doi.org/10.3389/fonc.2018.00170

Lai S, Wang P, Gong J, Zhang S (2023): New insights into the role of GSK-3β in the brain: from neurodegenerative disease to tumorigenesis. Peer J. **11,** e16635 https://doi.org/10.7717/peerj.16635

Lee E, Kazerooni EA (2022): Lung cancer screening. Semin. Respir. Crit. Care Med. **43,** 839-850 https://doi.org/10.1055/s-0042-1757885

Li Y, Lin Y, Tang Y, Jiang M, Chen X, Chen H, Nie Q, Wu J, Tong X, Li J et al. (2024): MAZ-mediated up-regulation of BCKDK reprograms glucose metabolism and promotes growth by regulating glucose-6-phosphate dehydrogenase stability in triple-negative breast cancer. Cell Death Dis. **15,** 516 https://doi.org/10.1038/s41419-024-06835-y

Li Y, Liu Y, Wang K, Xue D, Huang Y, Tan Z, Chen Y (2023): STK24 Promotes progression of LUAD and modulates the immune microenvironment. Mediators Inflamm. **2023,** 8646088 https://doi.org/10.1155/2023/8646088

Liu W, Zhou H, Wang H, Zhang Q, Zhang R, Willard B, Liu C, Kang Z, Li X, Li X (2022): IL-1R-IRAKM-Slc25a1 signaling axis reprograms lipogenesis in adipocytes to promote diet-induced obesity in mice. Nat. Commun. **13,** 2748 https://doi.org/10.1038/s41467-022-30470-w

Maity G, Haque I, Ghosh A, Dhar G, Gupta V, Sarkar S, Azeem I, McGregor D, Choudhary A, Campbell DR, et al. (2018): The MAZ transcription factor is a downstream target of the oncoprotein Cyr61/CCN1 and promotes pancreatic cancer cell invasion via CRAF-ERK signaling. J. Biol. Chem. **293,** 4334-4349 https://doi.org/10.1074/jbc.RA117.000333

Mederos N, Friedlaender A, Peters S, Addeo A (2020): Gender-specific aspects of epidemiology, molecular genetics and outcome: lung cancer. ESMO Open **5,** e000796 https://doi.org/10.1136/esmoopen-2020-000796

Mosaoa R, Kasprzyk-Pawelec A, Fernandez HR, Avantaggiati ML (2021): The mitochondrial citrate carrier SLC25A1/CIC and the fundamental role of citrate in cancer, inflammation and beyond. Biomolecules **11,** 141 https://doi.org/10.3390/biom11020141

Nasim F, Sabath BF, Eapen GA (2019): Lung cancer. Med. Clin. North Am. **103,** 463-473 https://doi.org/10.1016/j.mcna.2018.12.006

Rajendra A, Anurag Kumar S, Gaurav M, Anand M, Neerupma D, Harsha K, Bhupesh S, Niraj Kumar J, Harish D, Kamal D, et al. (2023): Diagnosis and clinical aspects of lung cancer: a special emphasis on drug targeting to cancer cells through nanoparticles. Lett. Drug Design Discov. **20,** 499-516 https://doi.org/10.2174/1570180819666220510133408

Rajpurohit H, Eiteman MA (2024): Citrate synthase variants improve yield of acetyl-CoA derived 3-hydroxybutyrate in Escherichia coli. Microb. Cell Fact. **23,** 173 https://doi.org/10.1186/s12934-024-02444-8

Samovski D, Jacome-Sosa M, Abumrad NA (2023): Fatty acid transport and signaling: mechanisms and physiological implications. Annu. Rev. Physiol. **85,** 317-337 https://doi.org/10.1146/annurev-physiol-032122-030352

Thommen DS, Koelzer VH, Herzig P, Roller A, Trefny M, Dimeloe S, Kiialainen A, Hanhart J, Schill C, Hess C, et al. (2018): A transcriptionally and functionally distinct PD-1(+) CD8(+) T cell pool with predictive potential in non-small-cell lung cancer treated with PD-1 blockade. Nat. Med. **24,** 994-1004 https://doi.org/10.1038/s41591-018-0057-z

Vazquez M, Carter D, Brambilla E, Gazdar A, Noguchi M, Travis WD, Huang Y, Zhang L, Yip R, Yankelevitz DF, et al. (2009): Solitary and multiple resected adenocarcinomas after CT screening for lung cancer: histopathologic features and their prognostic implications. Lung Cancer **64,** 148-154 https://doi.org/10.1016/j.lungcan.2008.08.009

Wang T, Zhu X, Wang K, Li J, Hu X, Lin P, Zhang J (2023): Transcriptional factor MAZ promotes cisplatin-induced DNA damage repair in lung adenocarcinoma by regulating NEIL3. Pulm. Pharmacol. Ther **80,** 102217 https://doi.org/10.1016/j.pupt.2023.102217

Wang W, Li D, Xu Q, Cheng J, Yu Z, Li G, Qiao S, Pan J, Wang H, Shi J, et al. (2024): G-quadruplexes promote the motility in MAZ phase-separated condensates to activate CCND1 expression and contribute to hepatocarcinogenesis. Nat. Commun. **15,** 1045 https://doi.org/10.1038/s41467-024-45353-5

Wang Y, Sun L, Qiu W, Qi W, Qi Y, Liu Z, Liu S, Lv J (2020): Inhibiting Forkhead box K1 induces autophagy to reverse epithelial-mesenchymal transition and metastasis in gastric cancer by regulating Myc-associated zinc finger protein in an acidic microenvironment. Aging (Albany NY) **12,** 6129-6150 https://doi.org/10.18632/aging.103013

Wei X, Li X, Hu S, Cheng J, Cai R (2023): Regulation of ferroptosis in lung adenocarcinoma. Int. J. Mol. Sci. **24,** 14614 https://doi.org/10.3390/ijms241914614

Wei ZW, Yang MZ, Yuan W (2024): Network pharmacological study of the active ingredient of panax notoginseng saponins for the treatment of lung cancer by inhibiting AKR1C3. Lett. Drug Design Discov. **21,** 1546-1554 https://doi.org/10.2174/1570180820666230914104206

Wu X, Gong L, Li B, Bai J, Li C, Zhang Y, Zhu H (2024): TNF-α can promote membrane invasion by activating the MAPK/MMP9 signaling pathway through autocrine in bone-invasive pituitary adenoma. CNS Neurosci. Ther. **30,** e14749 https://doi.org/10.1111/cns.14749

Xiao T, Li X, Felsenfeld G (2024): The Myc-associated zinc finger protein epigenetically controls expression of interferon-γ-stimulated genes by recruiting STAT1 to chromatin. Proc. Natl. Acad. Sci. USA **121,** e2320938121 https://doi.org/10.1073/pnas.2320938121

Yang HH, Jiang HL, Tao JH, Zhang CY, Xiong JB, Yang JT, Liu YB, Zhong WJ, Guan XX, Duan JX, et al. (2022): Mitochondrial citrate accumulation drives alveolar epithelial cell necroptosis in lipopolysaccharide-induced acute lung injury. Exp. Mol. Med. **54,** 2077-2091 https://doi.org/10.1038/s12276-022-00889-8

Yang Q, Lang C, Wu Z, Dai Y, He S, Guo W, Huang S, Du H, Ren D, Peng X (2019): MAZ promotes prostate cancer bone metastasis through transcriptionally activating the KRas-dependent RalGEFs pathway. J. Exp. Clin. Cancer Res. **38,** 391 https://doi.org/10.1186/s13046-019-1374-x

Yang Y, He J, Zhang B, Zhang Z, Jia G, Liu S, Wu T, He X, Wang N (2021): SLC25A1 promotes tumor growth and survival by reprogramming energy metabolism in colorectal cancer. Cell Death Dis. **12,** 1108 https://doi.org/10.1038/s41419-021-04411-2

You X, Huang L, Huang O, Deng Y, Shi X (2023): A comprehensive analysis of SLC25A1 expression and its oncogenic role in pan-cancer. Discov. Oncol. **14,** 207 https://doi.org/10.1007/s12672-023-00830-z

Yu ZH, Lun SM, He R, Tian HP, Huang HJ, Wang QS, Li XQ, Feng YM (2017): Dual function of MAZ mediated by FOXF2 in basal-like breast cancer: Promotion of proliferation and suppression of progression. Cancer Lett. **402,** 142-152 https://doi.org/10.1016/j.canlet.2017.05.020

Zeng J, Zhang L, Huang L, Yu X, Han L, Zheng Y, Wang T, Zhang N, Yang M (2024): MAZ promotes thyroid cancer progression by driving transcriptional reprogram and enhancing ERK1/2 activation. Cancer Lett. **602,** 217201 https://doi.org/10.1016/j.canlet.2024.217201

Zhang G, Wu J, Ji M, Liu X, Shi M (2025): SLC25A1 promotes lymph node metastasis of esophageal squamous cell carcinoma by regulating lipid metabolism. Int. J. Oncol. **66,** 15 https://doi.org/10.3892/ijo.2025.5721

Zhang H, Zhai X, Liu Y, Xia Z, Xia T, Du G, Zhou H, Franziska Strohmer D, Bazhin AV, Li Z, et al. (2023): NOP2-mediated m5C modification of c-Myc in an EIF3A-dependent manner to reprogram glucose metabolism and promote hepatocellular carcinoma progression. Research (Wash. DC) **6,** 0184 https://doi.org/10.34133/research.0184

Zhang H, Zhang P, Lin X, Tan L, Wang Y, Jia X, Wang K, Li X, Sun D (2024): Integrative single-cell analysis of LUAD: elucidating immune cell dynamics and prognostic modeling based on exhausted CD8+ T cells. Front. Immunol. **15,** 1366096 https://doi.org/10.3389/fimmu.2024.1366096

Zhang L, Hu W, Qiu Z, Li Z, Bian J (2023): Opportunities and challenges for inhibitors targeting citrate transport and metabolism in drug discovery. J. Med. Chem. **66,** 9229-9250 https://doi.org/10.1021/acs.jmedchem.3c00179

Zhang R, Peng X, Du JX, Boohaker R, Estevao IL, Grajeda BI, Cox MB, Almeida IC, Lu W (2023): Oncogenic KRASG12D reprograms lipid metabolism by upregulating SLC25A1 to drive pancreatic tumorigenesis. Cancer Res. **83,** 3739-3752 https://doi.org/10.1158/0008-5472.CAN-22-2679

Zhang Z, Qiao Y, Sun Q, Peng L, Sun L (2023): A novel SLC25A1 inhibitor, parthenolide, suppresses the growth and stemness of liver cancer stem cells with metabolic vulnerability. Cell Death Discov. **9,** 350 https://doi.org/10.1038/s41420-023-01640-6

Zheng C, Wu H, Jin S, Li D, Tan S, Zhu X (2022): Roles of Myc-associated zinc finger protein in malignant tumors. Asia Pac. J. Clin. Oncol. **18,** 506-514 https://doi.org/10.1111/ajco.13748

Received: February 14, 2025
Final version accepted: August 18, 2025

doi: 10.4149/gpb_2025036

**Supplementary Material**

# Upregulation of SLC25A1 by MAZ reprograms fatty acid synthesis and fuels LUAD malignancy

Xiaomeng Li[1] and Jing Li[1]

[1] *Respiratory Medicine Center, Weifang People's Hospital, Weifang, China*

## Supplementary Figure

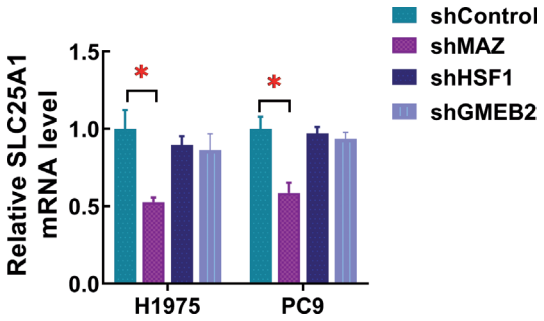



**Figure S1.** Effect of knockdown of MAZ, HSF1 or GMEB2 on SLC25A1 expression. H1975 and PC9 cells were randomly divided into four groups: shControl, shMAZ, shHSF1, and shGMEB2, with each group being transfected with the corresponding plasmid vectors according to the experimental design. qRT-PCR was employed to assess the expression levels of SLC25A1 in each group of cells.